Natural killer cell immunosuppressive function requires CXCR3-dependent redistribution within lymphoid tissues.

Ayad Ali, Laura M. Canaday, H. Alex Feldman, Hilal Cevik, Michael T. Moran, Sanjeeth Rajaram, Nora Lakes, Jasmine A. Tuazon, Harsha Seelamneni, Durga Krishnamurthy, Eryn Blass, Dan H. Barouch, Stephen N. Waggoner

SUPPLEMENTAL METHODS

Mice: C57BL/6, *Cxcr3*^{KO}, B6.SJL-*Ptprc*^{a}*Pepc*^{b}/BoyJ (Ly5.1), and B6.129S7-*Rag1*$^{tm1.1Cgn}$/J (*Rag*^{KO}) mice were purchased from Jackson Laboratory (Bar Harbor, ME). SMARTA LCMV-specific TCR transgenic mice (1) were a gift from Shane Crotty (La Jolla, CA) and bred to Ly5.1 mice in house. All mice were created or rigorously backcrossed onto the C57BL/6 background prior to receipt. Male mice between 8 to 20 weeks of age were routinely utilized in experiments. Mice were housed under barrier conditions and experiments performed under ethical guidelines approved by the Institutional Animal Care and Use Committees of Cincinnati Children's Hospital Medical Center. Staff were blinded to genotype and treatment status of experimental groups during harvesting, processing, and data acquisition.

Virus and viral vector injections*:* Mice were infected with the Armstrong strain of LCMV via intraperitoneal injection of $5x10^4$ plaque forming units per mouse. Viral stocks were previously generated in house (2) via propagation on BHK21 cells with titer determined using Vero cells (3). Other mice were given an intraperitoneal injection of $3x10^7$ plaque forming units of adenovirus serotype 5 (Ad5)-LacZ (a gift from Jeff Molkentin, Cincinnati, OH) or $1x10^{10}$ viral particles of Ad5-LCMV GP (from Dan Barouch, Boston, MA).

Mixed bone marrow chimeric mice: Mixed bone marrow chimeric (BMC) mice deficient in or expressing CXCR3 were generated by admixing the donor bone marrow of *Rag*^{KO}*Cxcr3*^{WT}

(referred to as CXCR3^{WT}) or *Rag^{KO}Cxcr3^{KO}* (referred to as CXCR3^{KO}) mice at a 9:1 ratio with bone marrow from wild-type Ly5.1 mice (4). In this mixture, NK cells and other innate lymphocytes preferentially derive from *Rag^{KO}* precursors while the adaptive compartment (T and B cells) can only develop from Ly5.1 precursors and as such are always *Cxcr3^{WT}*. Bilateral femur bones of mice were harvested and stripped of muscle tissue using gauze sponges and blades. Femur heads were cut to allow thorough flushing of the bone marrow with phosphate-buffered saline into a petri dish using a 10 mL syringe topped with a 26G needle. Bone marrow cells were counted using a hemocytometer and a bone marrow cell suspension was prepared to achieve 10x10^6 cells/mouse. Recipient C57BL/6 mice were lethally irradiated (See Irradiation) prior to intravenous injection of mixed bone marrow cells. A minimum of 16 weeks was allotted for reconstitution prior to initiating experimental infections.

SMARTA transfer model: SMARTA mouse spleens were harvested and processed into single cell suspensions (See Flow Cytometry) from which CD4 T cells were enriched by depletion of non-CD4 T cells (Miltenyi Biotec, Germany). 5x10^5 CD4 T cells were injected retro-orbitally into CXCR3^{WT}, CXCR3^{KO} and NK cell-depleted mice 1 day prior to LCMV infection. Six days following infection, spleens were harvested and SMARTA$^+$ CD4 T cell numbers, activation status and cytokine production were assessed by flow cytometry following in vitro LCMV-GP$_{64-80}$ (GPDIYKGVYQFKSVEFD) peptide stimulation (synthesized by 21st Century Biochemicals, Marlborough, MA).

Irradiation: Irradiation of mice was performed using the J. L. Shepherd Mark I Cesium Irradiator. Gamma irradiation was provided by Cesium 137 Source. Mice were placed into a rotating pie-shaped holder to limit mobility and ensure equal irradiation. The pie-shaped holder was then placed in the irradiator to deliver the required dose at a dose rate of 0.5 Gy per minute. The

optimal dose for hematopoietic ablation C57BL/6 mice is 11.75 Gy. All lethal doses/ablative doses were delivered as two split exposures to limit non-hematopoietic toxicity. The split exposures of 7.0 Gy for first exposure and 4.75 Gy for the second were separated by 3 hours. No anesthesia or analgesics were used in this procedure.

Intravascular staining: Protocols for intravascular staining of lymphocytes (5) were adapted to permit staining of NK cells. A few minutes prior to harvest, mice were anesthetized with isoflurane then given retro-orbital injections of 1.2 μg of rat anti-NKp46-APC (29A1.4, BioLegend, San Diego, CA) or goat anti-NKp46 (AF2225, R&D Systems, Minneapolis, MN) antibodies in 200 μL saline per mouse. The injected antibody was allowed to circulate for no more than 3 minutes prior to euthanasia. Spleens were then harvested, processed, and stained as described under flow cytometry or prepared for confocal imaging as described under tissue processing, sectioning and immunohistochemistry.

In vivo NK-cell depletion, recombinant IFN-α and IFNAR-1 blockade: One or two days before infection, selective depletion of NK cells (6) was achieved through a single intraperitoneal injection of 25 μg mouse anti-NK1.1 monoclonal antibody (PK136) or 25 μg of a control mouse IgG2a isotype antibody (C1.18.4) produced by Bio-X-Cell (West Lebanon, NH). At time of Ad5-GP or Ad5-LacZ vector immunization and for the two subsequent days, some mice were given intraperitoneal injections of 8 μg/mouse of recombinant interferon-α (752806, BioLegend, San Diego, CA). Similarly, on days 0, 1, and 2 of LCMV infection, IFN-I signaling was blocked via intraperitoneal injection of 400 μg of mouse anti-IFNAR-1 (MAR1-5A3) antibody from Bio-X-Cell (West Lebanon, NH). In other experiments, mice were given one intraperitoneal injection of 100 μg anti-IFNAR-1 antibodies at time of LCMV infection.

RNA Isolation, cDNA synthesis and RT-qPCR: Spleens harvested from mice were processed into single cell suspensions as described below (Flow Cytometry). 30 mg of whole spleen RNA was extracted via 30 second homogenization in RLT lysis buffer containing 1% β-mercaptoethanol per RNeasy kit (Qiagen, Germany). RNA was reverse transcribed into cDNA using iScript cDNA synthesis kit (BioRad, Hercules, CA). Subsequent RT-qPCR was performed using Taqman Gene Expression Assays (Applied Biosystems, Foster City, CA) to detect *Cxcl9* (Mm00434946_m1), *Cxcl10* (Mm00445235), *Cxcl11* (Mm00444662_m1), *Ifna9* (Mm00833983_s1), *Ifnb1* (Mm00439552_s1) and *Gapdh* (Mm99999915_g1). cDNA was combined with primers and Taqman Fast Advance master mix (ThermoFisher Scientific, Whaltham, MA) and amplified using Applied Biosystems 7500 Real-Time PCR and 7500 software v2.3.

Flow cytometry and in vitro peptide stimulation: Single-cell leukocyte suspensions were prepared from spleens by mechanical homogenization of tissues between frosted glass microscope slides (VWR, Radnor, PA) and filtration through a 70 µm nylon mesh. Following lysis of red blood cells, cells were plated at $2x10^6$/well in 96-well round-bottom plates, then either immediately subjected to flow staining or first stimulated for 5 hours at 37°C with 1 µM LCMV-GP_{64-80} peptide (GPDIYKGVYQFKSVEFD, 21st Century Biochemicals, Marlborough, MA) in the presence of brefeldin A (BD Biosciences, San Jose, CA). Leukocytes were then washed and resuspended in FACS buffer (Phosphate buffer saline + 5% fetal bovine serum + 0.5 mM EDTA) prior to surface staining with the following antibodies: CD3e (145-2C11), CD19 (1D3), TCRβ (H57-597), NKp46 (29A1.4), NK1.1 (PK136), CD49b (DX5), CD4 (GK1.5), CD8α (53-6.7), CD44 (IM7), CD43 (1B11), TCRVα2 (B20.1), CD45.1 (A20), CD45.2 (104), CXCR3 (CXCR3-173), Fas (SA367H8) IgD (11-26c.2a), GL7 (GL7), NKG2D (1D11), KLRG1 (2F1/KRLG1), NKG2A

(16A11), CD94 (18d3), Ly49H (3D10), DNAM-1 (TX42.1), CD11b (M1/70), CD27 (LG.3A10), CD25 (PC61) and granzyme B (GB11). All antibodies were purchased from BioLegend (San Diego, CA) or BD Biosciences (San Jose, CA). Cells were surface stained for 15 to 30 minutes at 4^{o}C. For CXCR3 staining, cells were incubated at room temperature. Following staining, cells were washed and fixed with BD fixation buffer (BD Biosciences, San Jose, CA) for 5 minutes at 4^{o}C. Cells were washed twice and resuspended in 200 μL FACS buffer. For intracellular staining, cells were washed and fixed with BD fixation/permeabilization buffer (BD Biosciences, San Jose, CA) for 15 to 20 minutes at 4^{o}C. Cells were then intracellularly stained with anti-IFN-γ (XMG1.2, BD Biosciences, San Jose, CA) and anti-TNF (MP6-XT22, BD Biosciences, San Jose, CA) for 15 to 30 minutes at 4^{o}C. Cells were then washed and resuspended in 200 μL FACS buffer and analyzed on a BD LSR Fortessa cytometer.

Tissue processing, sectioning, and immunohistochemistry: Tissues to be analyzed by fluorescence microscopy were placed into 4% formaldehyde solution for 5 hours followed by overnight dehydration in a 30% sucrose (Sigma-Aldrich, St. Louis, MO) solution at 4^{o}C. Samples were washed with phosphate buffered saline prior to embedding within optimal cutting temperature (OCT) media (Sakura Finetek, Maumee, OH) and frozen using a dry ice slurry in 100% ethanol and stored in -20^{o}C. Tissues were sectioned (7-10 μm thick) using a cryostat (Leica CM3050 S) and affixed to positively charged Denville slides (Thomas Scientific, Swedesboro, NJ). Slides were dried at room temperature for 5 to 10 minutes preceding a 10 minute fixation in chilled 100% acetone at -20^{o}C. Slides were subsequently dried at room temperature for 5 to 10 minutes and washed twice in chilled phosphate-buffered saline before being placed in saturation buffer containing 10% normal donkey serum (Sigma-Aldrich, St. Louis, MO) and 0.1% Triton-X (Sigma-Aldrich, St. Louis, MO) in phosphate buffered saline for blocking

at room temperature for 45 minutes. Slides were incubated with a primary antibody cocktail containing one or more of the following antibodies overnight at 4^{o}C: 1:100 goat anti-NKp46 (R&D Systems, Minneapolis, MN), 1:200 hamster anti-CD3e-AF594 or AF647 (500A2, BioLegend, San Diego, CA) and rat anti-CD169-AF594 or AF647 (3D6.112, BioLegend, San Diego, CA). The following day, slides were washed twice in chilled phosphate buffered saline. Subsequent secondary antibody staining with 1:1000 donkey anti-goat AF488 (Abcam, United Kingdom) was used for 2 hours at room temperature to reveal NKp46 primary staining. Slides were again washed twice with chilled phosphate buffered saline, mounted with prolong diamond mounting media (Thermo-Fisher Scientific, Waltham, MA), covered with a coverslip, and allowed to cure overnight prior to imaging.

Confocal microscopy & NK-cell quantification: Confocal imaging was performed using a Laser Scanning Nikon A1RSi Inverted Confocal Microscope with NIS Elements Confocal software. Z-stacked tissue images were acquired through a 10X objective (Nikon Plan Apo λ) from which a maximum intensity projection was generated prior to cell enumeration. Using tools available in NIS Elements Analysis software and guided by CD169- and CD3-staining, borders around white pulp (CD169 boundary) and T cell zones (CD3 boundary) were drawn. B220- and CD3-staining were used to delineate borders when enumerating NK cells within lymph nodes. NK cells located with these borders were enumerated using unbiased NIS Elements-derived algorithms and plotted using GraphPad Prism (San Diego, CA). To calculate NK cell proportions within the white pulp or T-cell zone, the total NKp46^{+} cells within the respective compartment were normalized to total NKp46^{+} cells within the field of view. Brightness and contrast for each representative image were adjusted equally across all channels using Photoshop CS6.

Statistics: Experimental results are consistently presented as the median with individual data point spread. Statistical differences between control and experimental groups were calculated using a one-way analysis of variance (ANOVA) with either the Holm-Šídák multiple comparison test or a Dunnett's multiple comparisons test. When a confidence interval was not desired, the Holm-Šídák multiple comparisons method was used to generate higher statistical power. A p-value of less than 0.05 was considered significant. Graphing and statistical analysis were routinely performed using GraphPad Prism (San Diego, CA). Researchers were blinded to groupings and treatment during experimental measurements.

REFERENCES

1. Oxenius A, Bachmann MF, Zinkernagel RM, and Hengartner H. Virus-specific MHC-class II-restricted TCR-transgenic mice: effects on humoral and cellular immune responses after viral infection. *European journal of immunology.* 1998;28(1):390-400.
2. Rydyznski C, Daniels KA, Karmele EP, Brooks TR, Mahl SE, Moran MT, et al. Generation of cellular immune memory and B-cell immunity is impaired by natural killer cells. *Nature communications.* 2015;6:6375.
3. Welsh RM, and Seedhom MO. Lymphocytic choriomeningitis virus (LCMV): propagation, quantitation, and storage. *Curr Protoc Microbiol.* 2008;Chapter 15:Unit 15A 1.
4. Kurtulus S, Sholl A, Toe J, Tripathi P, Raynor J, Li KP, et al. Bim controls IL-15 availability and limits engagement of multiple BH3-only proteins. *Cell death and differentiation.* 2015;22(1):174-84.
5. Anderson KG, Mayer-Barber K, Sung H, Beura L, James BR, Taylor JJ, et al. Intravascular staining for discrimination of vascular and tissue leukocytes. *Nature protocols.* 2014;9(1):209-22.
6. Waggoner SN, Cornberg M, Selin LK, and Welsh RM. Natural killer cells act as rheostats modulating antiviral T cells. *Nature.* 2012;481(7381):394-8.

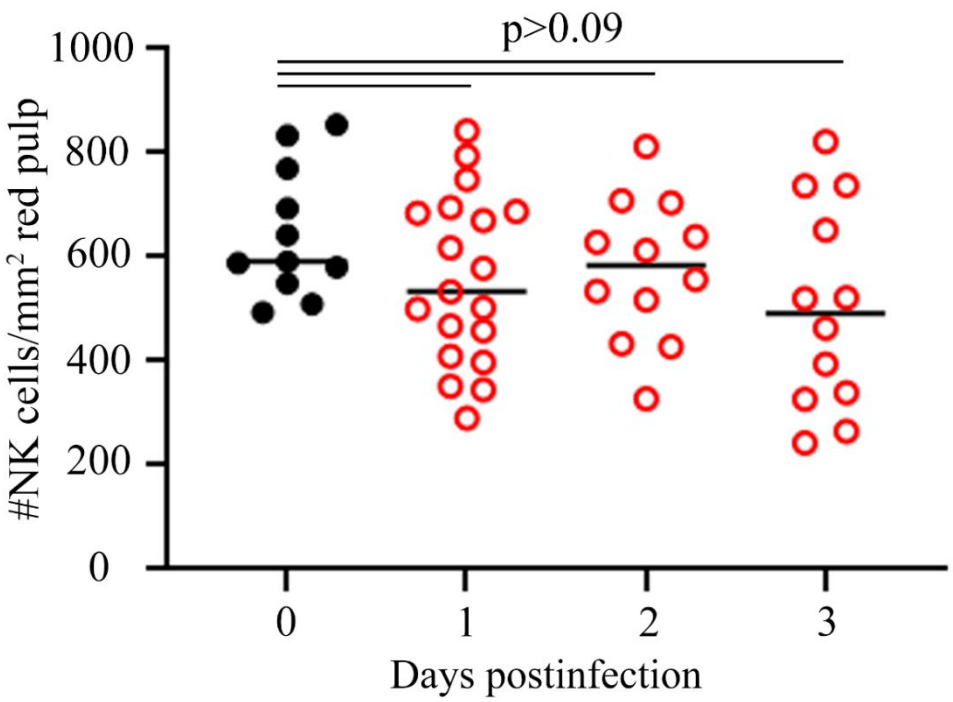

Supplemental Figure 1. Enumeration of NKp46^{+} NK cells within the splenic red pulp following infection. C57BL/6 mice (n=3-4/group) were infected with LCMV. At the indicated time-point post infection, the number of NKp46^{+} NK cells were enumerated by confocal imaging (see Figure 1) within the splenic red pulp defined by the region not bound the CD169 macrophages (5-12 follicles/mouse). Data are representative of two independent experiments. Statistical differences determined by one-way ANOVA.

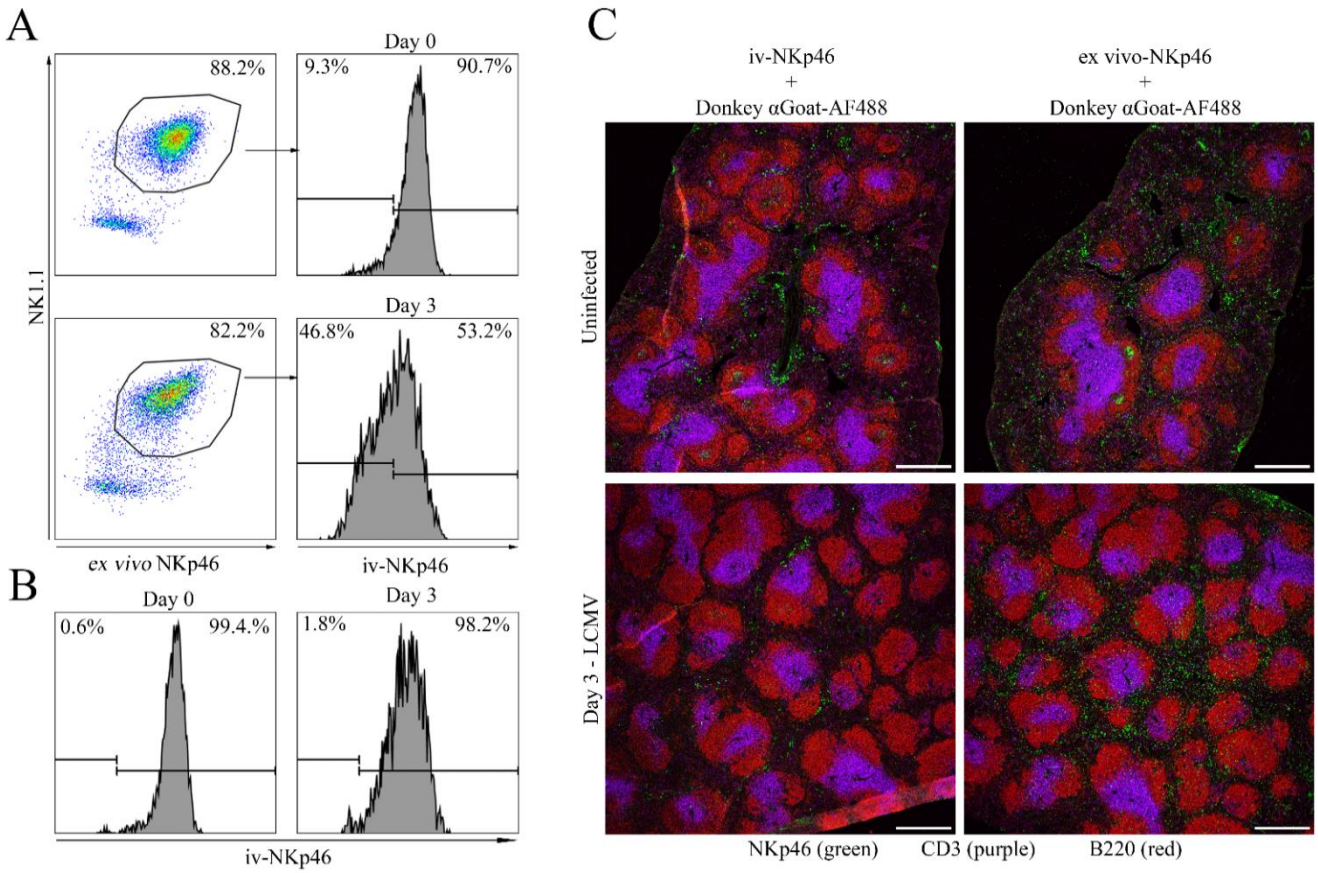

Supplemental Figure 2. Ex vivo and in vivo NKp46 staining in blood and spleen NK cells. C57BL/6 mice (n=3) were infected with LCMV prior to intravascular staining at indicated time points. (A) Representative plots showing gating of NK1.1^{+} ex-vivoNKp46^{+} NK cells among CD3^{neg} TCRβ^{neg} CD8α^{neg} CD49b^{+} spleen cells while representative histograms show iv-NKp46 staining on gated NK cells. (B) Representative plots show iv-NKp46 staining on NK cells (CD3^{neg} TCRβ^{neg} CD8α^{neg} CD49b^{+} NK1.1^{+} ex-vivoNKp46^{+}) in blood. (C) Representative confocal images of spleen sections from uninfected mice and infected mice 3 days following LCMV injection visualizing NKp46^{+} (green) NK cells, B220^{+} (red) B cells and CD3^{+} (purple) T cells following staining with either donkey anti-goat-AF488 secondary antibody alone or re-stained with goat anti-mouse anti-NKp46 antibody ex vivo prior to donkey anti-goat secondary. Scale bars measure 500 μm. Data are representative of two independent experiments.

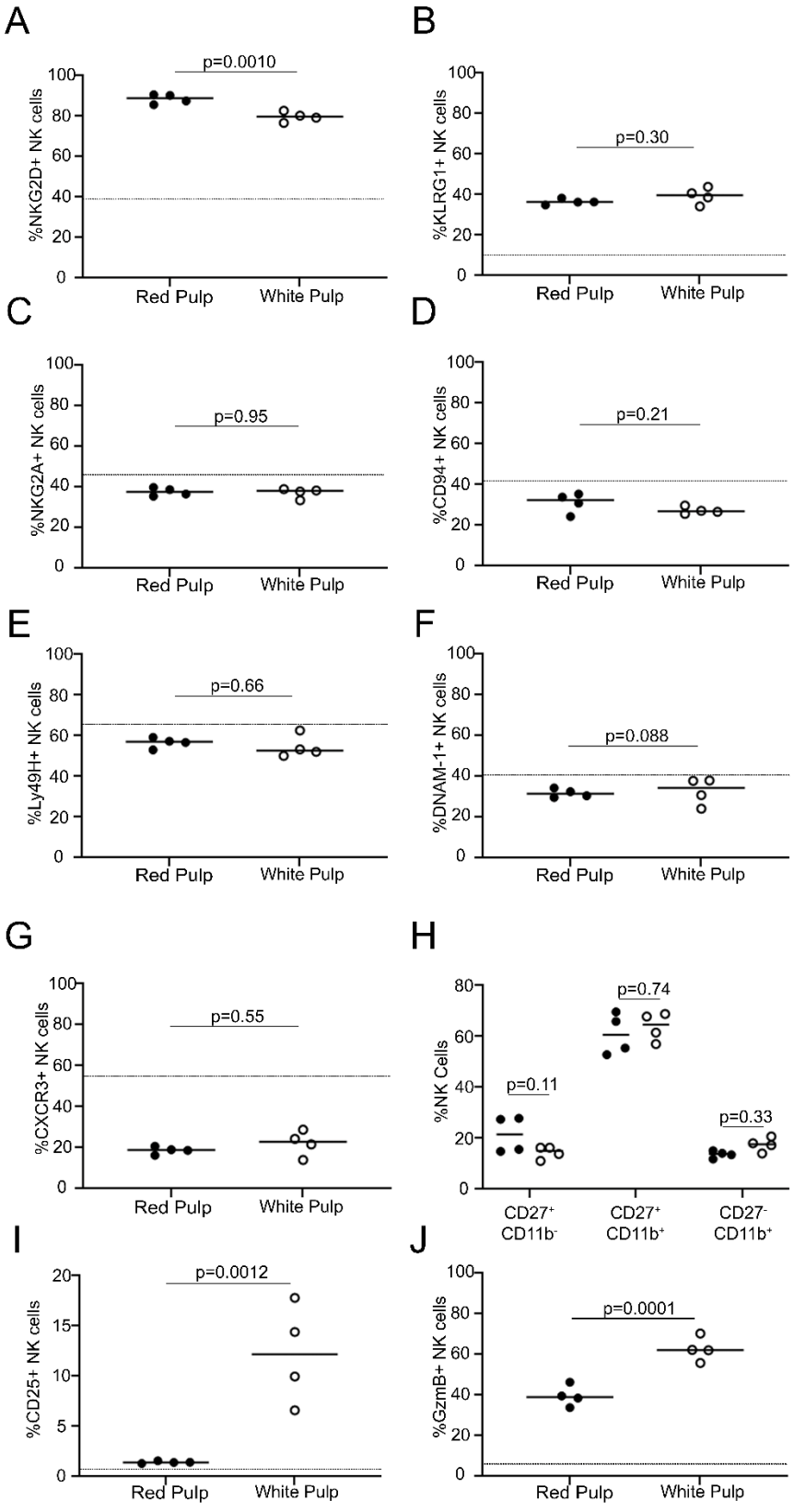
A
p=0.0010
%NKG2D+ NK cells
Red Pulp
White Pulp
B
p=0.30
%KLRG1+ NK cells
C
p=0.95
%NKG2A+ NK cells
D
p=0.21
%CD94+ NK cells
E
p=0.66
%Ly49H+ NK cells
F
p=0.088
%DNAM-1+ NK cells
G
p=0.55
%CXCR3+ NK cells
H
p=0.74
p=0.11
p=0.33
%NK Cells
CD27+ CD11b-
CD27+ CD11b+
CD27- CD11b+
I
p=0.0012
%CD25+ NK cells
J
p=0.0001
%GzmB+ NK cells

Supplemental Figure 3. Characterization of red pulp and white pulp-localized NK cells. (A-K) Three days following LCMV infection, C57BL/6 (n=4) mice were intravenously injected with anti-NKp46 antibody three minutes prior to euthanasia to label splenic NK cells ($CD3^{neg}$ $TCR\beta^{neg}$ $CD8\alpha^{neg}$ $CD49b^{+}$ $NK1.1^{+}$ ex-vivo$NKp46^{+}$) in vascularized red pulp (iv-$NKp46^{+}$) or white pulp (iv-$NKp46^{neg}$) regions. Cells were stained for the indicated markers and assessed by flow cytometry. The proportion of white pulp or red pulp NK cells expressing the indicated markers is shown. Dotted line reflects expression level in uninfected mice. Data reflect one of two independent experiments with statistical differences determined by Student's T-test.

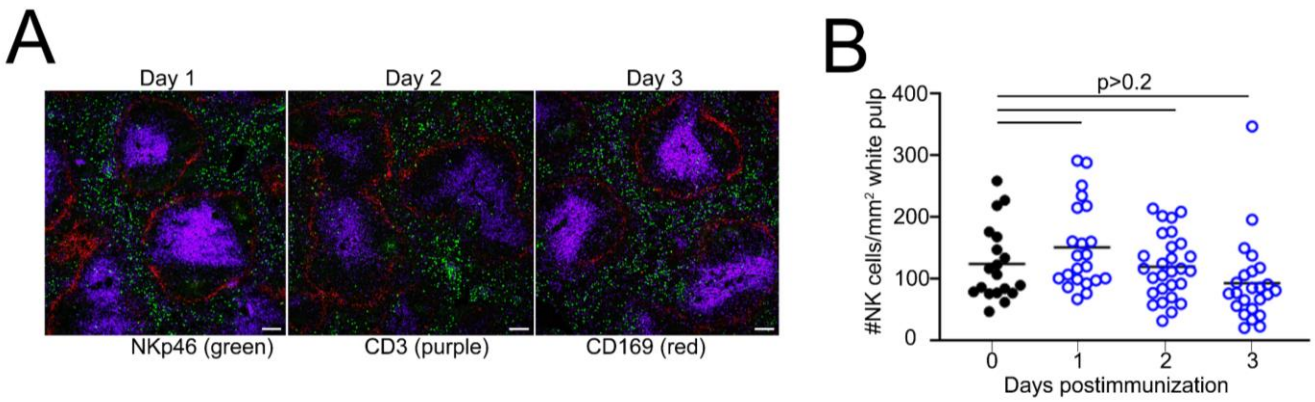

192

193 **Supplemental Figure 4. Splenic NK cell migration during adenoviral vector immunization.**

194 C57BL/6 mice (n=3-4) were inoculated with Ad5-LaZ. (A) At indicated times post inoculation,

195 spleens were imaged to determine localization of NKp46^{+} NK cells (green) relative to CD169^{+}

196 macrophages (red) and CD3 T cells (purple). (B) NK cells within the CD169-constrained white

197 pulp were enumerated in 5-12 follicles/mouse. Scale bars measure 100 μm. Data reflect one of

198 two independent experiments with statistical differences determined by one-way ANOVA.

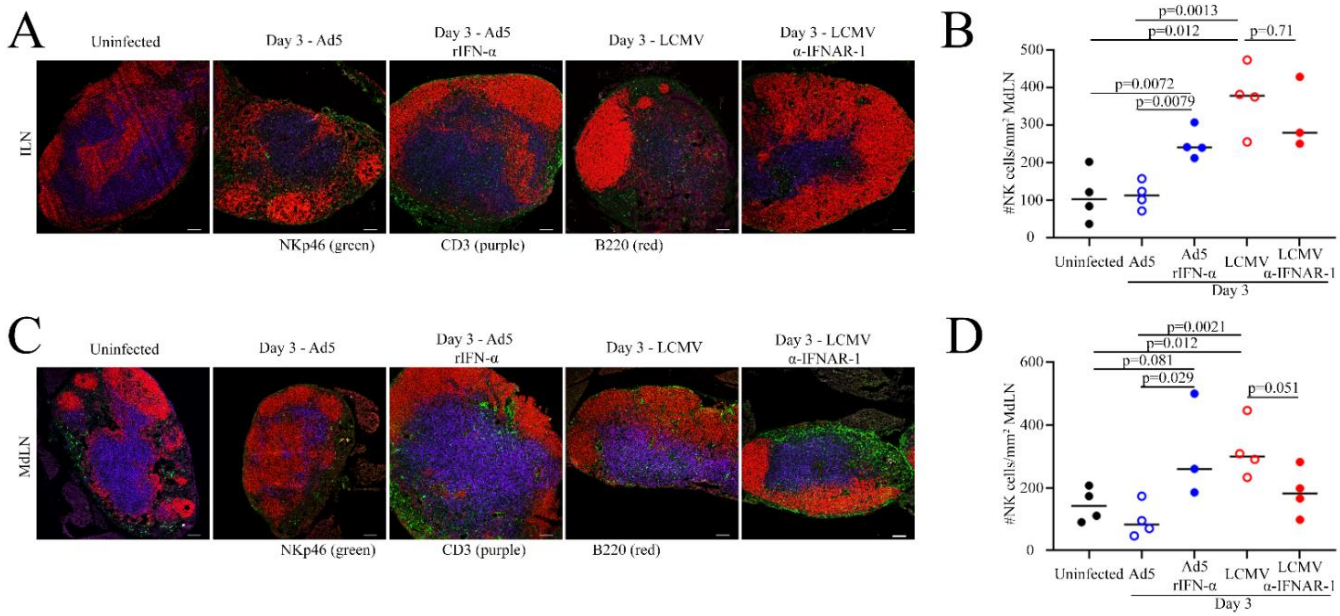

Supplemental Figure 5. Role of type I interferons in NK-cell localization in draining lymph nodes. C57BL/6 mice (n=3-4/group) were inoculated with Ad5-LacZ or LCMV and treated with either 8 μg/mouse recombinant IFN-α or 400 μg/mouse anti-IFNAR-1 antibodies. On day 3 of infection, NKp46^{+} (green) NK cells were enumerated within the B220^{+} (red) and CD3^{+} (purple) zones of inguinal (A-B) and mediastinal (C-D) lymph nodes. Data reflect one of two independent experiments with statistically significant differences determined by one-way ANOVA. Scale bars measure 100 μm.

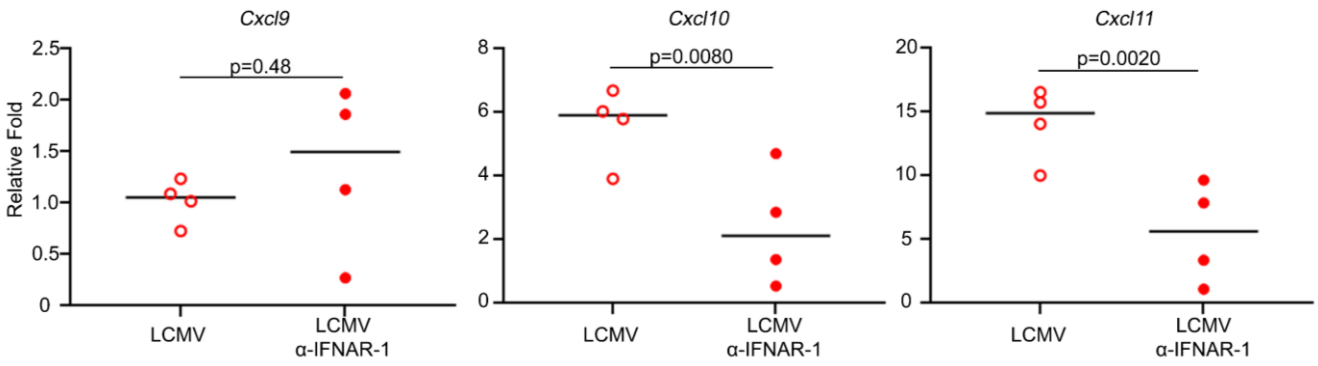

Supplemental Figure 6. Reduced CXCR3 ligand expression following IFNAR blockade during LCMV infection. C57BL/6 mice (n=4/group) were treated or not with 100 μg anti-IFNAR antibodies prior to LCMV infection. Two days following infection, spleens were harvested, and mRNA was extracted for RT-qPCR analysis of *Cxcl9, Cxcl10,* and *Cxcl11* expression levels. Statistical differences determined by Student's T-test. Data are representative of two independent experiments.

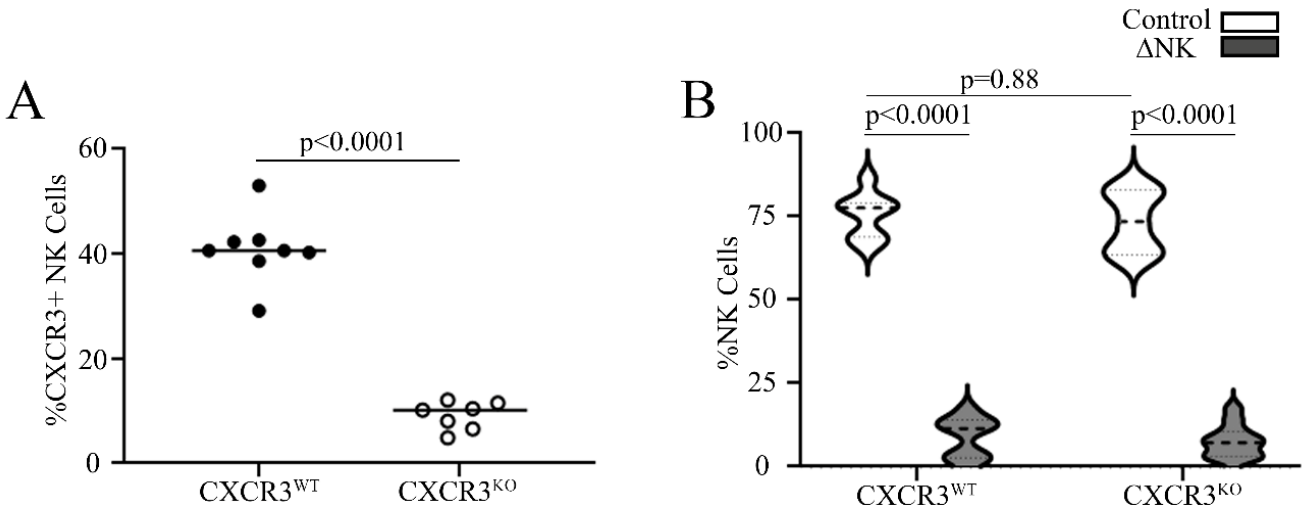

215

216 **Supplemental Figure 7. Confirmation of NK cell depletion and CXCR3 deletion in NK cells.**

217 Proportion of (A) CXCR3^{+} or (B) total CD49b^{+} NKp46^{+} NK1.1^{+} NK cells 7 days post-infection in

218 mixed CXCR3^{WT} or CXCR3^{KO} bone-marrow chimeras (n=7-12) depleted or not of NK cells. Data

219 pooled from two independent experiments with statistically significant differences determined by

220 (A) Student's T-test or (B) one-way ANOVA.

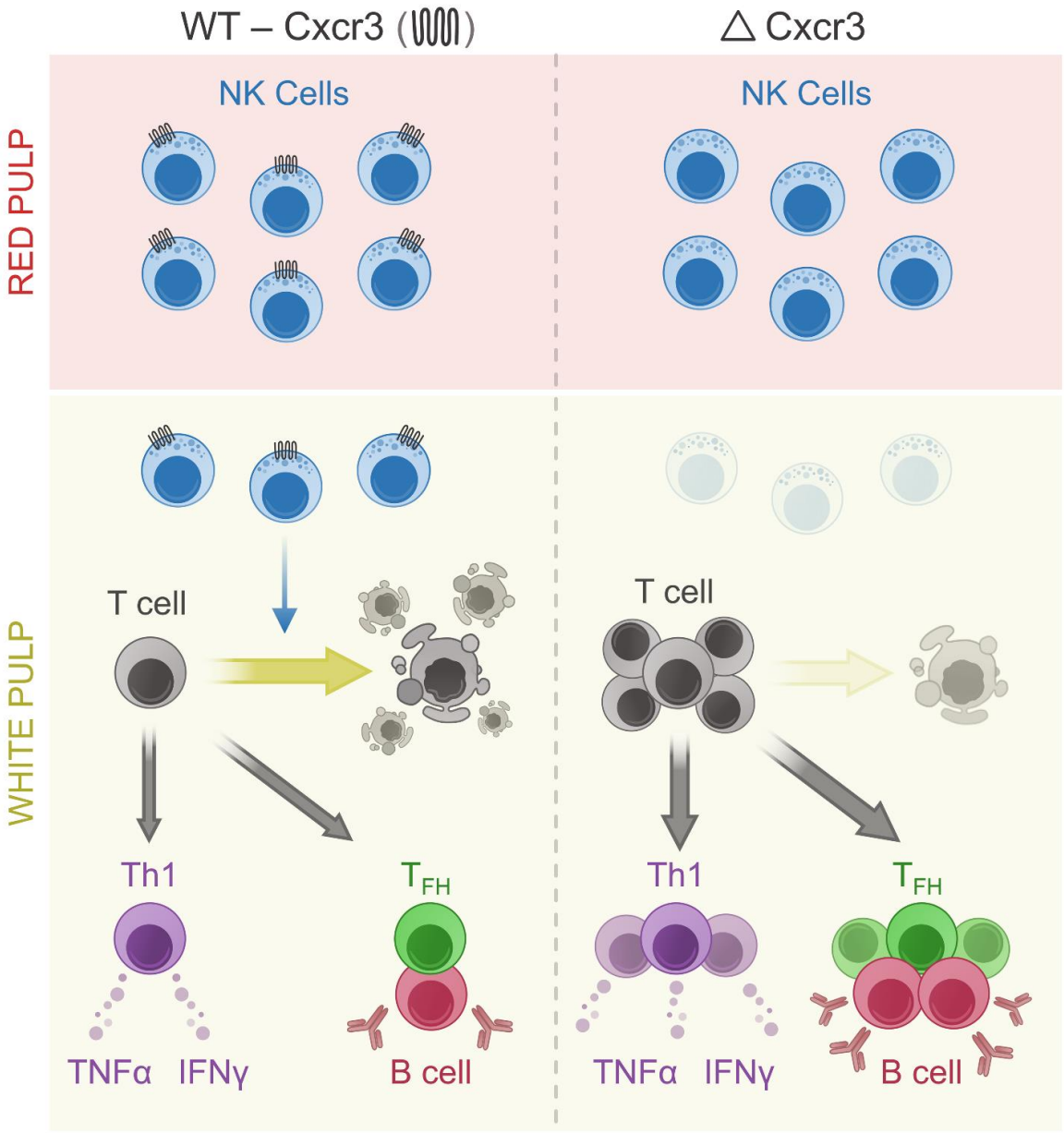

Supplemental Figure 8. Model of CXCR3-dependent NK cell immunoregulatory activity during infection. Viral infection leads to NK cell localization within T cell-rich follicles wherein they cull antiviral T cells, diminishing T cell cytokine responses and generation of T_{FH} cells. We propose that loss of CXCR3 on NK cells impairs this localization, rescuing T cells from NK cell-driven death. CXCR3 deletion thereby allows for increased T cell cytokine responses and T_{FH} cell generation important for viral control and antibody production.